Estuarine, Coastal and Shelf Science 83 (2009) 379–391

Contents lists available at ScienceDirect

Estuarine, Coastal and Shelf Science

journal homepage: www.elsevier.com/locate/ecss

Sediment segregation by biodiffusing bivalves

F. Montserrat [a,b,*], C. Van Colen [c], P. Provoost [b], M. Milla [b], M. Ponti [d], K. Van den Meersche [b,c], T. Ysebaert [b,e], P.M.J. Herman [b]

[a] Delft University of Technology, Faculty of Civil engineering and Geosciences, Hydraulics Section, P.O. Box 5048, 2600 GA Delft, The Netherlands
[b] Netherlands Institute of Ecology, Centre for Estuarine and Marine Ecology, Korringaweg 7, 4401 NT, Yerseke, The Netherlands
[c] Ghent University, Marine Biology Department, Krijgslaan 281 – S8, B-9000, Ghent, Belgium
[d] Centro Interdipartimentale di Ricerca per le Scienze Ambientali in Ravenna (CIRSA), University of Bologna, Via S. Alberto 163, 48100 Ravenna, Italy
[e] Wageningen IMARES, P.O. Box 77, 4400 AB Yerseke, The Netherlands

ARTICLE INFO

Article history:
Received 4 February 2009
Accepted 3 April 2009
Available online 18 April 2009

Keywords:
intertidal
cohesive
sediment
sand
mud
erosion
deposition
luminophores
image analysis
bioturbation
ecosystem engineering

ABSTRACT

The selective processing of sediment fractions (sand and mud; >63 μm and ≤63 μm median grain size) by macrofauna was assessed using two size classes of inert, UV-fluorescent sediment fraction tracers (luminophores). The luminophores were applied to the sediment surface in 16 m^2 replicated plots, defaunated and control, and left to be reworked by infauna for 32 days. As the macrofaunal assemblage in the ambient sediment and the control plots was dominated by the common cockle *Cerastoderma edule*, this species was used in an additional mesocosm experiment. The diversity, abundance and biomass of the defaunated macrobenthic assemblage did not return to control values within the experimental period. Both erosion threshold and bed elevation increased in the defaunated plots as a response to the absence of macrofauna and an increase in microphytobenthos growth. In the absence of macrobenthos, we observed an accretion of 7 mm sediment, containing ca. 60% mud. Image analysis of the vertical distribution of the different luminophore size classes showed that the cockles preferentially mobilised fine material from the sediment, thereby rendering it less muddy and effectively increasing the sand:-mud ratio. Luminophore profiles and budgets of the mesocosm experiment under "no waves–no current" conditions support the field data very well.

1. Introduction

Intertidal soft sediments are governed in their dynamics (e.g. erosion, deposition, transport) by both physical and biological processes (Borsje et al., 2008; Daborn et al., 1993; Nowell et al., 1981; Rhoads, 1974). Intertidal sediments consist of a mixture of gravel, sand and mud. Mud (<63 μm), in turn, consists of a mixture of silt (quartz powder) and clay where for a particular estuarine system, the ratio between silt and clay is constant and in accordance with the specific hydrodynamic energy conditions (Flemming, 2000). A sediment matrix built up of coarse sediment particles (sand and gravel) in contact with each other displays a granular behaviour. Gradually increasing the mud content of such a matrix will cause the interstitial spaces to be filled up and the sand particles to lose contact with each other. Once the matrix is dominated by mud instead of by sand particles, the sediment behaviour will change from non-cohesive to cohesive; the sediment will behave less granular and more like a firm gel (Van Ledden, 2003; Winterwerp and Van Kesteren, 2004). As mud (clay) strongly influences mechanical properties like the cohesiveness of the sediment and thus erosive behaviour (Dade et al., 1992; Mitchener and Torfs, 1996; Van Ledden et al., 2004), coastal and estuarine sediment transport and morphology can differ with different mud contents.

Besides being ca. two orders of magnitude smaller than sand, clay particles are not spherical but consist of layered platelets. Their shape and size give them a high specific surface area and an electrical charge which interacts with ambient (water and organic) molecules and other particles (Winterwerp and Van Kesteren, 2004). The sediment mud content is therefore positively correlated with organic matter (OM) content (Hedges and Keil, 1995) and respiration and mineralisation rates (Aller, 1994), but also with other biogeochemical characteristics such as the capacity to bind heavy metals and other pollutants (Bouezmarni and Wollast, 2005). In sediment beds dominated by mud, cohesive forces between the

* Corresponding author. Netherlands Institute of Ecology, Centre for Estuarine and Marine Ecology, Korringaweg 7, 4401 NT, Yerseke, The Netherlands.
E-mail address: f.montserrat@nioo.knaw.nl (F. Montserrat).

0272-7714/$ – see front matter © 2009 Elsevier Ltd. All rights reserved.
doi:10.1016/j.ecss.2009.04.010

particles are dominant as sand and silt particles are captured in a clay–water matrix.

In coastal lagoons, estuaries and tidal basins, the main physical drivers for sediment mud content are hydrodynamic energy gradients (Oost, 1995; Van Ledden, 2003). Classical hydrodynamic models which treat sand-mud segregation in coastal areas do not incorporate biological processes (Van Ledden, 2003). Even the most recent state-of-the-art morphodynamic models which recognise that small-scale benthic biologically-mediated processes reflect in large-scale sediment dynamics, have a grid size in the order of km and a sub-grid level in the order of 200–800 m (Borsje et al., 2008). Unless averaged over the grid cells, these models cannot account for small- to mid-scale biological processes which can cause sharp boundaries between sandy and muddy areas in nature and create a patchy intertidal landscape (Van De Koppel et al., 2001).

Benthic animals can change the sediments' erodability autogenically (i.e. by their own physical structures; Luckenbach, 1986; Montserrat et al., 2008; Van Duren et al., 2006) or allogenically (i.e. bioturbation; Andersen et al., 2002; Rhoads and Young, 1970; Willows et al., 1998). Also, by modifying the composition (i.e. the sand:mud ratio), organisms can alter the sediments' geomechanical properties like cohesiveness and erosion threshold (Le Hir et al., 2007; Winterwerp and Van Kesteren, 2004). For example, biodeposition is a process in which suspension-feeding fauna capture fine sediment fractions from the water column and deposit them nearby as (pseudo)faeces (Haven and Morales-Alamo, 1966; Oost, 1995). If this material is not immediately resuspended, the surrounding sediment will become muddier, organically enriched and more cohesive. Benthic invertebrates are also known to cause incorporation or expulsion of fine sediment fractions through bioturbation (Volkenborn et al., 2007a), respectively, bioventilation or bioresuspension (De Deckere et al., 2000). Differential processing of sediment fractions through bioturbation is a process that can change the sediment composition and have profound consequences for its biogeochemistry (Volkenborn et al., 2007b).

In order to study bioturbation processes numerous tracer techniques have been developed over the last three decades (Maire et al., 2008), including the use of phaeopigment concentration profiles (Gerino et al., 1998), radionuclides (Andersen et al., 2000; Mulsow et al., 2002; Sandnes et al., 2000; Wheatcroft and Martin, 1996), inert fluorescent sediment tracers called luminophores (Gerino, 1990; Mahaut and Graf, 1987) and even silver and gold (Wheatcroft et al., 1994). Especially the use of luminophores has taken a flight in bioturbation studies. Here, luminophores are used to model and quantify vertical particle transport and to estimate biodiffusion coefficients (D_b) of both single species (Duport et al., 2006; Maire et al., 2007) and of multi-species communities (Duport et al., 2007; Gilbert et al., 2007). The luminophores have been applied in frozen "cakes" or as a layer either at the sediment surface, at a certain depth or both (Caradec et al., 2004) to distinguish between transport directions. Solan et al. (2004) combined the use of luminophores with an *in situ* time-lapse sediment profile camera, obtaining a series of cross-sectional images of the sediment in which both the reworking of tracer and natural benthic activity were captured. In all abovementioned cases only one size class of luminophore was used. To our knowledge and as mentioned in a review by Maire et al. (2008), there have been no studies in which two or more size classes of luminophores were deployed to study particular bioturbation processes. Here, we did use two size classes of luminophores, each as a tracer for the sediment fractions mud (<63 μm) and sand (>63 μm and < 2000 μm), to determine selectivity between sediment fractions by bioturbating macrofauna.

The focus of this study is to assess the temporal and spatial scale of bioturbation of a natural benthic community and one that has been removed. To investigate the net bioturbatory effect of a intertidal benthic community we used defaunation to exclude the effect of macrobenthos *in situ* following the exact same method and spatial scale as was done in Van Colen et al. (2008) and Montserrat et al. (2008). Our hypothesis is that the net effect of the macrofaunal assemblage is removing the fine sediment fraction, to yield less muddy sediment, with a consequent lower erosion threshold. To test our hypothesis, i.e. to detect possible differential processing of sediment fraction tracers and resulting possible changes in sand:mud ratio in this field experiment, we used two size classes of luminophores, each with a different colour, as conservative sediment fraction (mud and sand) tracers.

In addition to the field experiment, we conducted a mesocosm experiment under controlled conditions, using the same sediment fraction tracers. In this mesocosm experiment we assessed the bioturbatory effects on sediment fraction segregation of the most important species in terms of biomass in the ambient sediment at the research site (Van Colen et al., 2008): the common cockle *Cerastoderma edule* Linnaeus (1758).

2. Materials and methods

2.1. Site, defaunation treatment and luminophore application

The experiment was conducted in an intertidal flat area (Paulinapolder) on the southern shore of the Westerschelde estuary (51°21′24″ N and 3°42′51″ E; SW Netherlands; Fig. 1a). Within this area, four 16 m^2 square plots were randomly chosen to be used in this study (Fig. 1b). Two plots were defaunated by covering the sediment in plastic foil, inducing severe hypoxia, for a period of 94 days. After this period, the plastic foil was cut open at the sediment surface, referred to as day 0. A vertical subsurface lining of plastic foil was left intact to prevent horizontal subsurface immigration of macrobenthic infauna. For more information and details about the exact defaunation method see Montserrat et al. (2008) and Van Colen et al. (2008). Two other 16 m^2 square plots consisted of untreated ambient sediment and were used as controls.

The fluorescent sediment tracers used (luminophores, i.e. fluorescent dyed thermoplastic polyamide powder, Environmental Tracing Systems, UK; http://www.environmentaltracing.com/) were coded "Magenta" and "UV Blue Mostyn" with a median grain size (D_{50}) of 41 μm and 129 μm, respectively. Overlap between the two fraction tracers existed in that the D_{90} of "Magenta" was 86 μm and the D_{10} of "UV Blue Mostyn" was 72 μm. Luminophores were volumetrically mixed in the ambient sand:mud ratio of the sediment and in turn volumetrically mixed 1:1 with sieved (1 mm) ambient sediment. The sediment–tracer mix was poured in plaster moulds of 25 × 25 × 0.5 cm and frozen at −20 °C to make sediment 'tiles'. At $t = 0$, the frozen tiles were then placed in a square of 2 × 2 tiles covering 0.25 m^2, both in the north-west and in the south-east corners, at ca. 1 m from the edges of the experimental plots (Fig. 1c).

2.2. Sampling

The experiment started on 23 May 2005 by opening the plastic sheeting (referred to as $t = 0$, see above). The plots were sampled at $t = 1$ h, 1 tide, 3 days, 7 days, 14 days and 32 days. The collection consisted of samples taken for luminophore analysis, macrobenthos abundance, macrobenthos biomass, erosion threshold and bed elevation. Samples were taken in quadrant 1 and 3 in each plot (i.e. two replicates per plot; Fig. 1c).

For luminophore sampling, cores made out of 30 cm long PVC pipes with an inner diameter of 36 mm and a wall thickness of 2 mm were used. To minimise compaction of the sediment while pushing down the core, a plunger of a 100 ml syringe was drawn

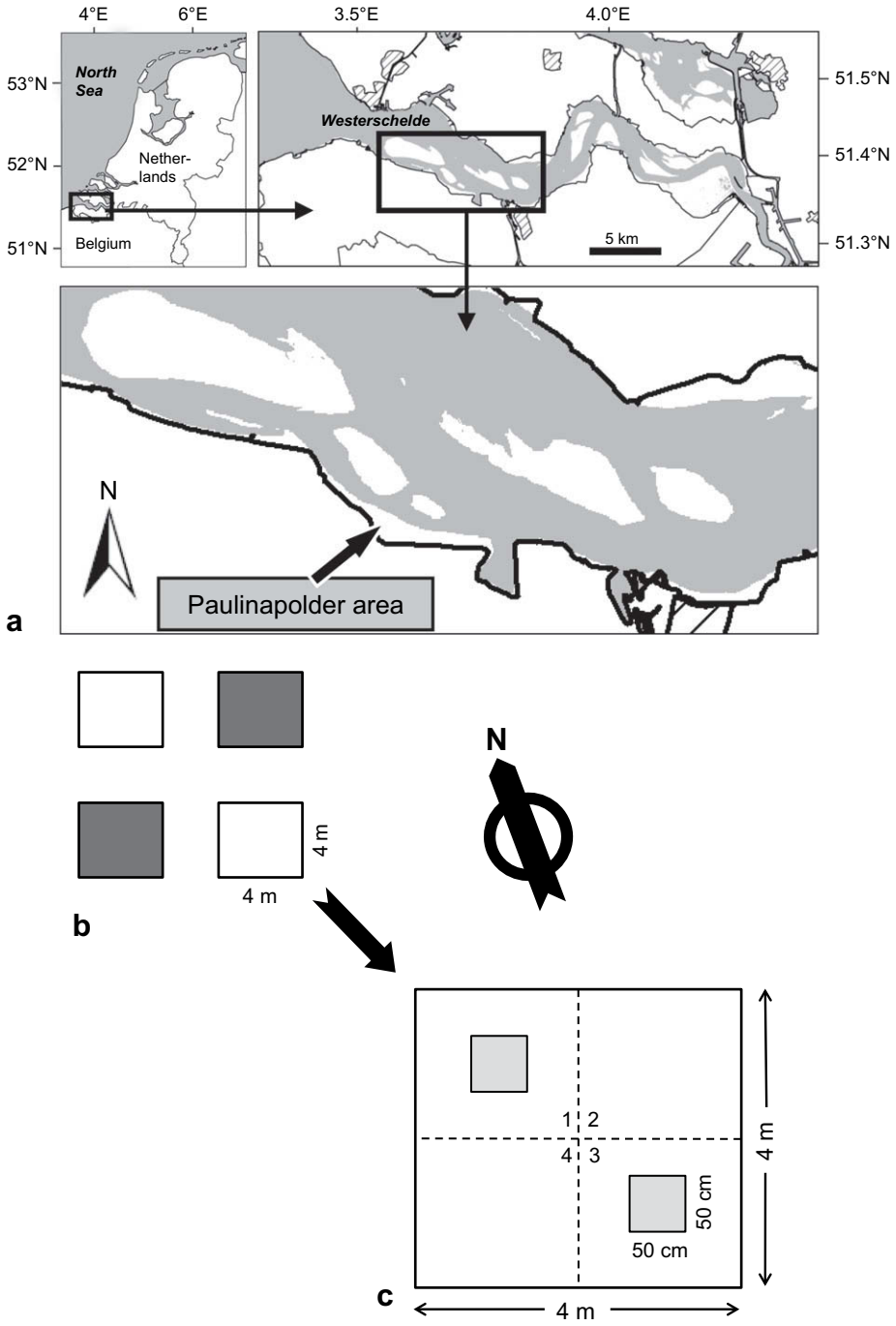

Fig. 1. (a) The geographic position of the research site within the polyhaline part of the Westerschelde estuary, SW Netherlands. (b) Schematic representation of the defaunated (dark) and control (light) replicated plots. Distance between plots is not to scale. (c) Schematic representation of the placement of the luminophore tiles in (grey) 50 × 50 cm squares.

upwards. Luminophore cores were stored on dry ice (approx. −70 °C) in the field to arrest macrofaunal reworking, taken to the lab and further stored at −20 °C until processing.

Macrofauna was sampled to a depth of 30 cm, using an 11 cm inner diameter stainless steel corer. Macrofauna samples were taken to the lab, sieved over a 1 mm sieve and preserved in a neutralised 4% formaldehyde solution with 0.01% Bengal Rose until processing. Macrofaunal biomass was determined according to Sistermans et al. (2007) and given in grams ash-free dry mass per square meter (g AFDM m^{-2}).

The sediment strength, or erosion threshold is taken as a measure of erodability of the sediment under a certain bottom shear, and was measured using a cohesive strength meter Mk III (CSM, Sediment Services, UK; Tolhurst et al., 1999). The measurements were performed according to the 'Mud 6' programme of the CSM Mk III.

The sediment bed level elevation was measured relative to NAP (=Normaal Amsterdams Peil; Amsterdam Ordnance Datum, similar to Mean Sea Level) according to Montserrat et al. (2008). Between five and eight replicate measurements were taken per sampled

quadrant. Bed level measurements were performed using a rotating laser mounted on a tripod (fixed at a point outside the experimental area) and a receiving unit on a portable measuring pole with a mm scale. There was evidence of baseline variability in the bed elevation measurements; to correct for this variability, the bed elevation values are given as the difference in elevation ± standard deviation (SD) between the defaunated and the control plots. Assuming there is no covariance between the treatments, the SD for the difference in bed elevation is calculated according to:

$$\sigma^2_{\text{defaunated-control}} = \sigma^2_{\text{defaunated}} + \sigma^2_{\text{control}}$$

The luminophore cores were taken from within the 0.25 m^2 tracer area (Fig. 1c). All other samples were taken from the adjacent sediment within the experimental plots, max. 30 cm away from the luminophore tiles. To prevent disturbance of the sediment profile, all holes left in the sediment after extraction of the respective variables were filled up with PVC tubes of the same diameter and length, which were closed at one side with duct tape.

2.3. Mesocosm experiment

In the mesocosm experiment, PVC cores (66 mm inner diameter, 2 mm wall thickness, 85 mm height) were filled with 1 mm sieved ambient sediment, of which half each received one live cockle drawn from a population with shell length 29.47 ± 2.35 mm (mean ± SD) and wet weight 9.64 ± 2.18 g (mean ± SD). Then, a 3 mm thick disc of frozen luminophore/sediment mix (∅ = 66 mm) was placed on top of the sediment in each experimental core. We replicated nine times to yield 18 cores in total. One-third, i.e. 3 "Cockle–No Cockle" (C–NC) pairs, was immediately frozen at −20 °C to serve as a $t = 0$ where no sediment reworking could have taken place. The remaining six replicates of C–NC pairs were placed within each of the six 8 dm^3 mesocosm units. Wave and/or current action generated by the simulated tidal water movement in the mesocosm units was negligible. After 21 days, the mesocosm experiment was terminated by removing all cores from the setup and placing them at −80 °C for 1.5 h, after which they were placed at −20 °C until processed.

2.4. Luminophore image analysis

Both the PVC cores used to extract material from the tracer-enriched sediment surface from the field and the PVC cores used in the mesocosm experiment were, while still frozen, longitudinally cross-sectioned using a band saw. The frozen smear left by the band saw was chafed away using a razor. Every half core was photographed in the light and in the dark under blacklight, using a digital mirror-reflex camera (Canon EOS 350D with 18–55 mm EFS objective) mounted on a stand. The images measured 2304 × 3456 pixels, and were saved using JPEG compression. The area photographed measured 43 × 67 mm, resulting in a resolution of 18.66 μm × 19.39 μm per pixel. The images were analyzed using custom-made Matlab scripts. First, the images were corrected for the uneven sediment surface. The corrected sediment surface was superimposed on the corresponding images taken in the dark, to vertically translate the pixel columns of the image accordingly. Subsequently, discriminant analysis was used to classify all pixels into one of the classes "red luminophores" (i.e. mud fraction mimic), "blue luminophores" (i.e. sand fraction mimic) or "background" (i.e. ambient sediment), based on their brightness values in the red, green and blue bands (each between 0 and 255). A training set was composed by manually selecting pixels pertaining to each of the three classes. The classification outcome was verified by comparing false-colour and original images. Finally, the number of pixels belonging to the different classes was determined for each pixel row.

2.5. Data analysis

All field results were analysed according to a Complete Randomised (CR) experimental design. We performed generalised linear modelling analysis of variance (GLM-ANOVA) to test for differences between time (i.e. sampling occasions), treatments, plots and, in the case of bed level measurements, quadrants. To ensure normal distribution of the residuals, visual inspection of Normal *P*-plots was performed. Macrofauna data were $(x+1)^{0.25}$ transformed in the case of abundance and $\ln(x+1)$ transformed in the case of biomass (Quinn and Keough, 2002).

The general linear model (GLM) for macrofauna (both for abundance and biomass) included Time and Treatment as separate fixed factors and Plot nested in Treatment with Plot as a random factor, plus the interaction terms Time × Treatment and Time × Plot nested in Treatment. The GLM for erosion threshold included Time, Treatment, Plot nested in Treatment and the interaction term Time × Treatment. Containing an extra source of variation, the GLM for bed level elevation included Time, Treatment, Quadrant nested in Plot nested in Treatment and the interactions terms Time × Treatment and Time × Quadrant nested in Plot nested in Treatment. Analyses on luminophore budgets from the field experiment were done using analysis of covariance (ANCOVA), with treatment as a covariate. Analyses of the sediment budgets from the lab experiment were done using a full-factorial ANOVA with Time, Treatment and Fraction, including all interaction terms as factors. All data analyses have been performed using R: a language and environment for statistical computing (R Development Core Team, 2007; Vienna, Austria; http://www.R-project.org).

3. Results

3.1. Field experiment – general observations

In similarly defaunated plots, used in a parallel experiment, the sediment was rendered azoic after 40 days of hypoxia (Montserrat et al., 2008; Van Colen et al., 2008). Therefore, in this experiment it was assumed that after 94 days of induced hypoxia all macrobenthos was dead and decomposed in the defaunated plots. The tracer tiles were placed in quadrants 1 and 3 (Fig. 1c) and all samplings were done after 1 h. Because of the warm weather, the tiles thawed very quickly. Shortly after placement on the control plots, various benthic animals (particularly cockles) would emerge from underneath the experimental tiles. After the sampling, when the tide returned, we observed the applied tracer tiles for several minutes and no significant amount of tracer was transported away from the plots. Also, when we returned to do the sampling after one tide, the tracer tiles were still very well visible. After two days, mini-ripples present on the ambient sediment (and thus also the control plots) had migrated over the tracer tiles (Fig. 2). These observations indicated that, after thawing, the tracer tiles became integrated with the ambient sediment matrix and did not cause or display any anomalous sediment behaviour.

3.2. Field experiment – benthic assemblage

Throughout the experimental period, both the total abundance and total biomass in the defaunated plots were at least an order of magnitude lower than in the control plots. Total macrofaunal abundance in the control plots ranged between 13 511 ± 624 ind. m^{-2} at day 0 and 8159 ± 3084 ind. m^{-2} at day 32, whereas that in the defaunated plots started at 245 ± 39 ind. m^{-2}

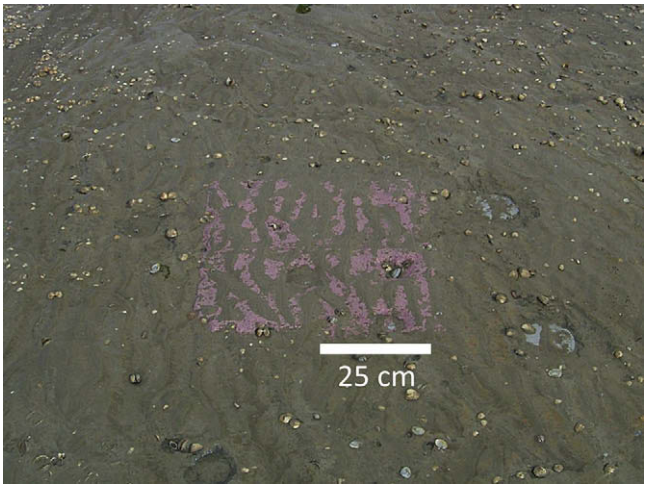

Fig. 2. A square of 2 × 2 luminophore tiles after 2 days in the field experiment. Note the sand ripples which migrated over the luminophore tiles, perpendicular to the tidal water movement.

and increased to 1579 ± 538 ind. m^{-2} at day 32. Total abundance was found to be different with significant effects of Time, Treatment and Time × Treatment interaction (Table 1). The total macrofaunal biomass in the control plots ranged between 110.82 ± 27 g AFDM m^{-2} at day 0 and 78.24 ± 38 g AFDM m^{-2} at day 32, whereas that in the defaunated plots amounted to 0.04 ± 0.02 g AFDM m^{-2} at day 0 and increased one order of magnitude to 0.51 ± 0.3 g AFDM m^{-2} at day 32. Total macrofaunal biomass was found to be different with significant effects of Time, Treatment, Plot nested in Treatment and Time × Treatment interaction.

There were seven species that accounted for 75–99 % of the total macrobenthic biomass in both treatments (Fig. 3). A conspicuous difference between the treatments was that in the control plots the bulk of the biomass was made up by adult *Cerastoderma edule*. Its biomass varied between 61% of the total community biomass at day 0 and 83% at day 32 (Fig. 3), while in the defaunated plots adult *C. edule* did not occur within the 32 day experimental period. Within the first week, the common Mudsnail, *Hydrobia ulvae* (Pennant, 1777) was – with 94% of the biomass at day 7 – the dominant species of the highly impoverished assemblage in the defaunated plots, whereas it never constituted more than 2.7% of the natural assemblage in the control plots. The contribution of *H. ulvae* to the total biomass in the defaunated plots decreased to ca. 40% towards day 32. Simultaneously, *Nereis* (=*Hediste*) *diversicolor* (Müller, 1776) started to recolonise the defaunated plots and contributed about 40% to the assemblage in the defaunated plots. Only at the end of the experimental period, freshly recruited, juvenile *Macoma balthica* (Linnaeus, 1758) contributed almost 14% to the total macrobenthic biomass in the defaunated plots, while in the control plots it remained stable around 15% throughout the entire period.

3.3. Field experiment – sediment characteristics

The sediment erosion threshold displayed different patterns between the treatments. The defaunated sediment had a higher erosion threshold than the control plots, albeit with a very high variability around the mean (Fig. 4a). In the control plots both the mean erosion threshold and variance were low. The greatest difference between the two treatments occurred at day 32. This difference in erosion threshold between the treatments coincided with a visible bloom of microphytobenthos in the defaunated plots (chl *a* data not shown here), as the surface sediment turned a dark brown as observed in Montserrat et al. (2008). Upon inspection of the Normal *P*-Plot of the erosion data, violation of the assumption of homoscedasticity was suspected. To correct for this, Quinn and Keough (2002) suggest square root $x+1$ transformation for data with right skew. GLM-ANOVA found only a significant effect of Treatment.

Table 1
Summary of the analysis of variance of the measured environmental (biotic and abiotic) variables. The first column (variable) states the analysed variable with its appropriate transformation in bold. In the second column (source of variation), the factors taken into the explanatory model for each variable can be found. The last column (*p*) states the *p*-value of the effect.

Variable	Source of variation	SS	df	MS	*F*	*p*
Total abundance macrofauna **fourth root($x+1$)**	Time	47.337	9	5.260	2.788	**0.0305**
	Treatment	412.625	1	412.625	108.590	**0.0091**
	Plot(Treat)	7.603	2	3.801	2.026	0.1602
	Time × Plot(Treat)	34.000	18	1.889	1.565	0.1226
	Time × Treat	95.521	9	10.613	5.626	**0.0009**
	Error	44.670	37	1.207		
Total biomass macrofauna **ln($x+1$)**	Time	74.865	9	8.318	4.2316	**0.0044**
	Treatment	512.682	1	512.682	55.3433	**0.0176**
	Plot(Treat)	18.536	2	9.268	4.7312	**0.0219**
	Time × Plot(Treat)	35.410	18	1.967	1.2961	0.2458
	Time × Treat	86.174	9	9.575	4.8709	**0.0021**
	Error	56.158	37	1.518		
Elevation **ln($x+1$)**	Time	125.09	8	15.64	2.4579	**0.0267**
	Treatment	38.86	1	38.86	0.0318	0.8644
	Quad(Treat × Plot)	7314.51	6	1219.08	191.6367	≪**0.0001**
	Time × Quad(Treat × Plot)	286.26	45	6.36	16.0367	≪**0.0001**
	Time × Treat	85.20	8	10.65	1.6742	0.1312
	Error	54.74	138	0.40		
Erosion threshold **square root($x+1$)**	Time	36.25	3	12.08	2.25	0.1448
	Treatment	146.79	1	146.79	27.36	**0.0004**
	Plot(Treat)	40.09	3	20.05	3.74	0.0614
	Time × Treat	4.44	2	1.48	0.28	0.8417
	Time × Plot(Treat)	12.68	3	4.23	0.79	0.5278
	Error	53.65	10	5.37		

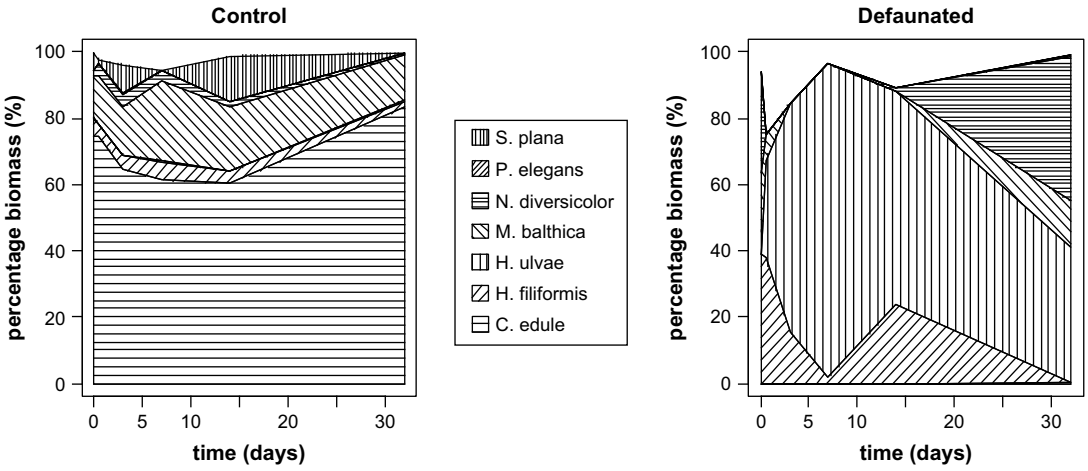

Fig. 3. The relative contribution to the total biomass in both treatments of the seven most abundant species. In the right hand panel (defaunated) there is a minor contribution of (juvenile) *C. edule* at the end of the experimental period and no contribution of *Scrobicularia plana*.

The sediment bed level elevation relative to NAP of the defaunated plots started somewhat lower than the control plots. From day 7 onwards, the bed level of the defaunated plots started to rise. At the same time a decrease in the bed level of the control plots was observed (ANCOVA: $p = 0.0072$ and $p = 0.0179$, respectively; Multiple $r^2 = 0.4174$). The difference in elevation of the defaunated plots increased to 4.2 mm above the control plots on day 32 (Fig. 4b). As the Normal *P*-Plot of the elevation data did not show any evidence of heteroscedasticity, the data were not transformed. There were significant effects for the factors Time, Quadrant nested in Treatment nested in Plot and Time × Quadrant nested in Treatment nested in Plot interaction, but not for Treatment or for Time × Treatment interaction. We explicitly refer to Table 1 for all results of the statistical analyses of abovementioned macrobenthos and sediment parameters.

On day 7, ca. 2 mm of material had accreted on top of the sediment in the defaunated plots (Fig. 5a and b). The accretion occurred in a linear fashion (linear regression: slope = 0.19 mm day^{-1}, $p = 0.0021$, multiple $r^2 = 0.9254$), reaching approximately 7 mm at day 32. The percentage of mud in the accreted material (Fig. 5c) also increased linearly, reaching around 60% at day 32, although this increase was not statistically significant (linear regression: slope = 0.36% day^{-1}, $p = 0.0587$, Multiple $r^2 = 0.3127$). At the same time in a parallel experiment, the top 1 cm of the ambient sediment contained 45% mud and similarly defaunated sediment contained ca. 50% mud (Montserrat et al., 2008).

3.4. Field experiment – luminophore profiles

The vertical profiles of the luminophores are shown in Fig. 6a–d. In the case of both the coarse and the fine tracer in the defaunated plots, we observed a subsidence of the layer of luminophores which is in effect the burial of the layer by accreted sediment (see above). The peak of the pixel count over the vertical can be seen to be gradually moving downwards (Fig. 6a and b). For both fractions of tracers within the defaunated plots, we clearly observed a loss of material over time. In one of the two control plots, a small amount of the coarse tracer (Fig. 6c) was already found at 1–1.5 cm depth after 1 h (0 days, first panel). At day 3, a slight diffusion of the luminophore layer to approx. 1 cm can be seen, but by day 7 and onwards, a rapid loss of material had occurred. Apart from the advection–diffusion transport processes, we did observe some non-local vertical

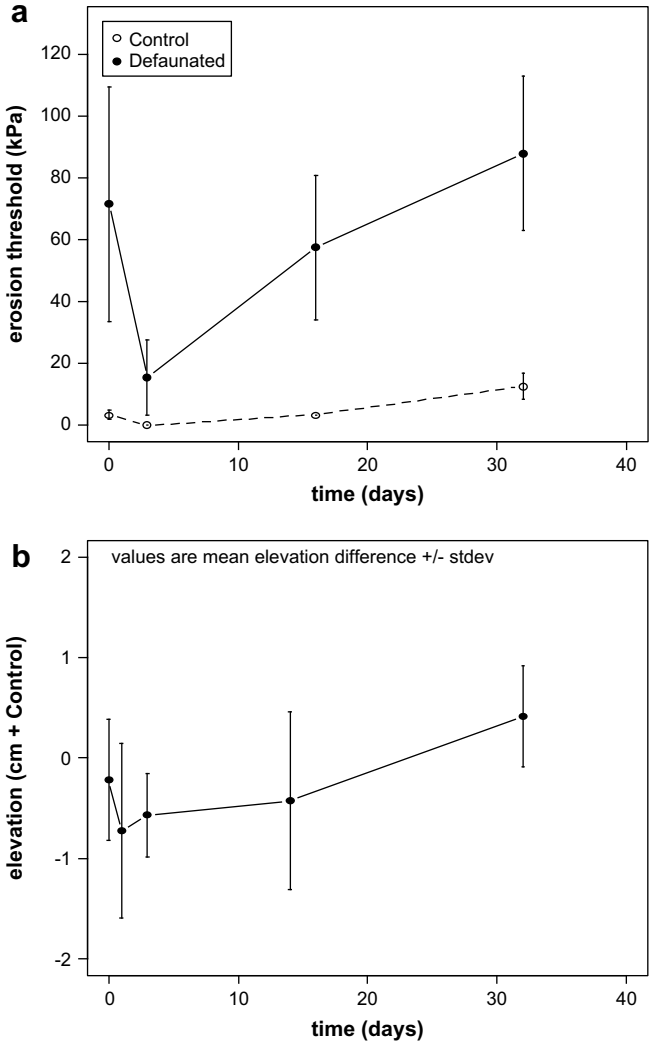

Fig. 4. (a) The mean ± SEM eroding pressure (measured with CSM Mk IV) in both treatments as a function of time. (b) The mean ± SD elevation difference of the defaunated plots, compared to the controls, in cm.

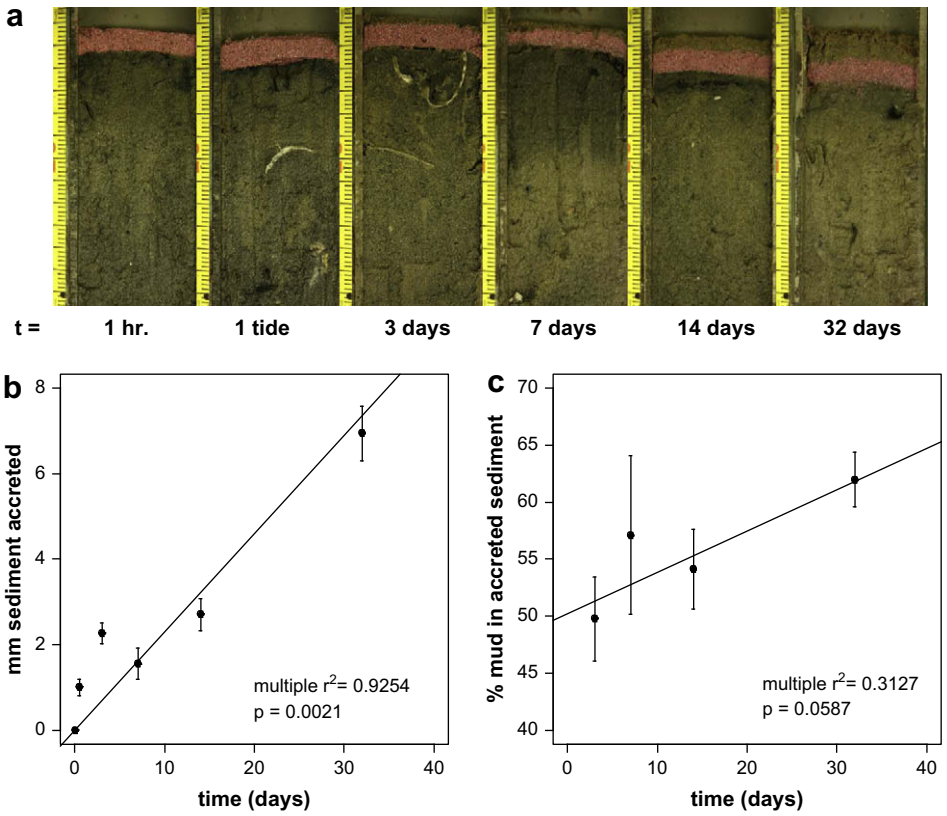

Fig. 5. (a) Longitudinally cross-sectioned cores containing sediment extracted from the defaunated plots, with a pink layer of sediment–luminophore mix. Each frame is representative of the cross sections of the cores during the mentioned sampling occasion (from left to right: $t = 0$, 1 tide, 3 days, 7 days, 14 days and 32 days, respectively). (b) The mean ± SEM amount of accreted material on top of the defaunated plots, in mm. The accreted material was measured from the underside of the luminophore layer. (c) The mean ± SEM percentage mud (sediment fraction ≤ 63 μm) in the accreted material on the corresponding sampling occasions, in %.

transport to depths up to ca. 1.5–2 cm (Figs. 6c, 7 days and 32 days). The fine tracer displayed a similar profile over time as it was quickly mixed to about 1 cm depth in one of the control plots, but was not found below that depth at subsequent samplings. At day 14 and day 32, only a small fraction of the initial amount of fine tracer was detected in the control plots.

3.5. Field experiment – sediment budgets

Depth-integrated pixel counts decreased for both tracer fractions in both treatments. In all cases there was a rapid decrease of material within the first four samplings (0–7 days), followed by a steady but much slower loss of material. In the control plots, almost 100% of the fine luminophores were lost by the end of the experiment. We regressed the natural log-transformed depth-integrated mean pixel count for both fraction tracers against Time with Treatment as a covariate (Fig. 7a). Between tracer fractions, the fine tracer was lost faster than the coarse tracer (ANCOVA: $p \ll 0.0001$). Starting from a full factorial (overparametrised) model containing Time, Treatment and Fraction, and all interactions as factors, the factors Treatment ($p = 0.1133$) and Treatment × Fraction did not have an effect ($p = 0.963$). Removal of both of these factors yielded a minimal adequate model (MAM): $\ln(\text{pixel}) = \text{Time} + \text{Fraction} + \text{Time} \times \text{Treatment} + \text{Time} \times \text{Fraction} + \text{Time} \times \text{Fraction} \times \text{Treatment}$, of which the parameter estimates are given in Table 2. The loss rates are significantly different between sampling occasions (Time) and between fractions, while the fraction-specific loss rate also differs between treatments.

Integrated over the top 3 cm of sediment, the tracer ratio of coarse:fine increased over time for both treatments. However, the coarse:fine ratio increased more rapidly for the control than for the defaunated plots (ANCOVA: $p \ll 0.0001$) during the experimental period (Fig. 7b). The coarse:fine luminophore ratio in the control plots increased from 15.1 to 113.5 (7.3 times), against an increase from 17.9 to 42.0 (2.35 times) in the defaunated plots.

3.6. Mesocosm experiment – profiles and budgets

The luminophore profiles of the experimental cores in the mesocosm experiment were similar to those extracted in the field experiment, albeit with obvious differences like the absence of accretion of sediment in the "No Cockle" (NC – comparable to "Defaunated") cores, and the consequent subsidence of the luminophore layer. Large parts of the luminophore layer on top of some of the NC cores were lost during processing. These cores were therefore omitted from the analysis. The cockles in the "Cockle" (C – comparable to "Control") cores were recorded moving, burrowing and 'shaking' (*sensu* Flach, 1996) or 'coughing' (rapid valve adductions), thereby expelling visible amounts of tracer which accumulated around the base of the cores during the experiment. In both the C and the NC cores which were immediately frozen (the "0 days" cores), no sediment reworking had occurred: both treatments displayed the same profiles for both tracer fractions (data not shown).

In the C and the NC cores, tracer material in the layer which constituted the initial luminophore disc (i.e. 0–3 mm) had disappeared from this layer after 21 days. However, the tracer profiles

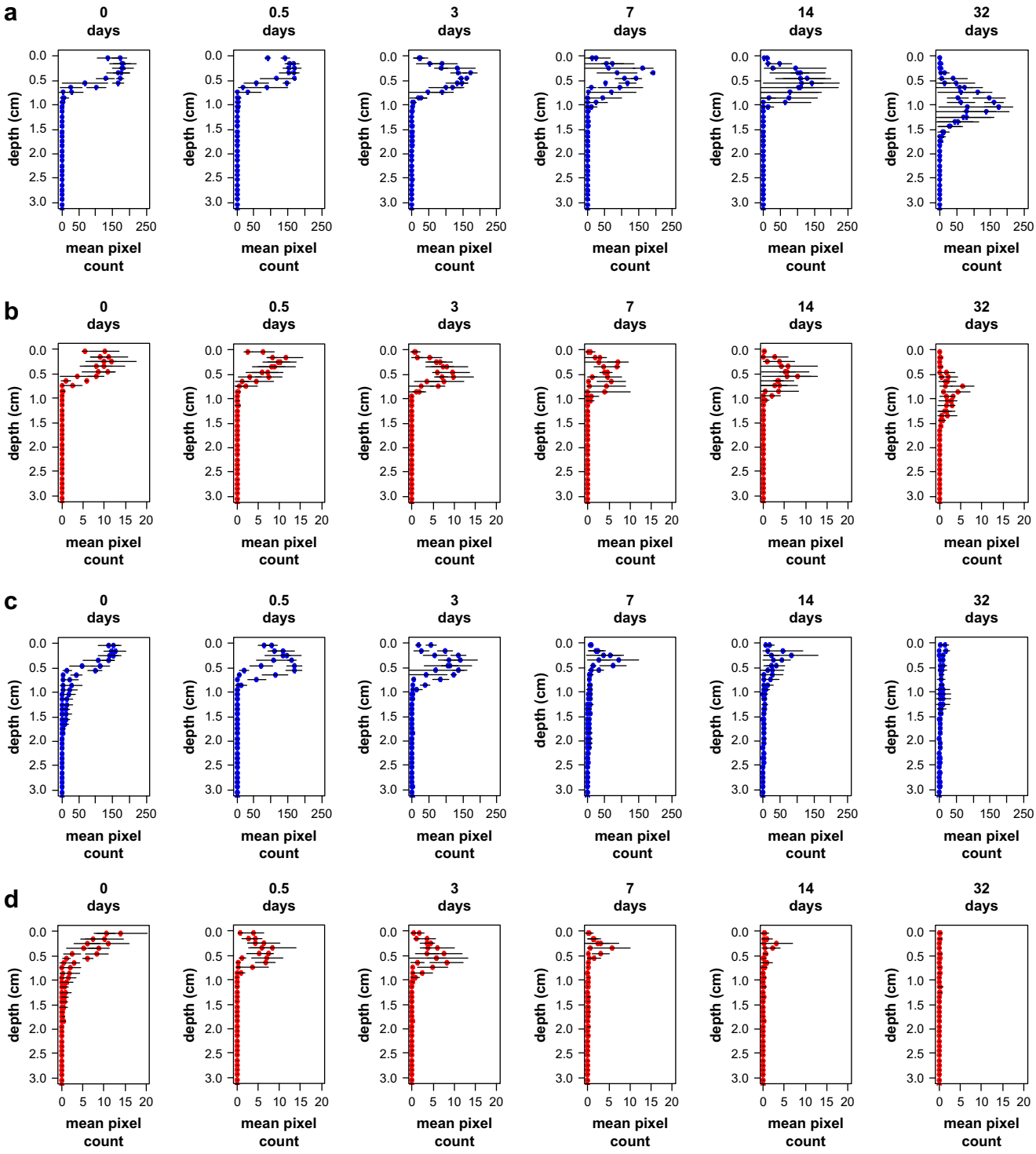

Fig. 6. Luminophore profiles as a function of sediment depth in the field defaunation experiment. The solid circles are the mean values per plot ($n = 2$) with the error bars representing the SEM (subquadrants per plot, $n = 2$). (a) Defaunated plots, coarse luminophores. (b) Defaunated plots, fine luminophores. (c) Control plots, coarse luminophores. (d) Control plots, fine luminophores.

of the NC cores were very similar to any of the "0 days" cores, in the sense that the initial luminophore layer was largely intact. The loss from the initial layer, the luminophore disc, in the NC cores was around 30% of the coarse tracer and 5% of the fine tracer (Fig. 8a and b). Compared to the C cores, the loss was 86% for the coarse and 89% for the fine tracer.

Besides expelling sediment, the cockles' movements also transported the tracer material downward into the sediment to form a three-layer system (Fig. 8c and d). Starting from the sediment surface the first layers (0 – 5.5 mm depth), being the remnants of the luminophore disc, consisted of 25% of the initial values for the coarse tracer and 17% of the initial values for the fine tracer (i.e. the luminophore disc at 0 days). A second, uniformly mixed layer started at 5.5 mm deep and continued to around 23.5 mm deep. This uniform layer consisted of 32% of the starting values for the coarse tracer and 9% of the initial values for the fine

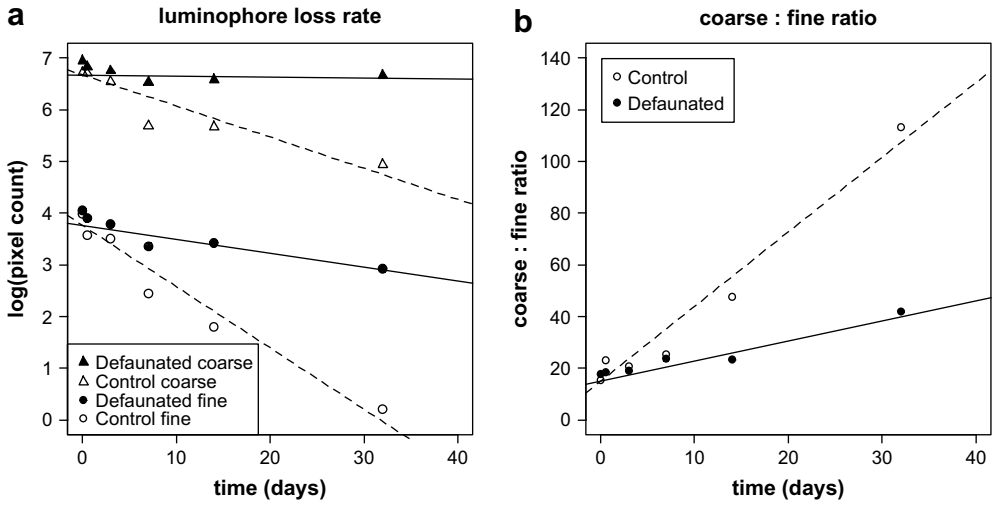

Fig. 7. The luminophore loss rate as a function of time. The *y*-axis denotes the natural log-transformed pixel count for the coarse luminophores (triangles) and for the fine luminophores (circles). The open symbols and the dashed lines represent the values and linear regression for the control plots, the solid black symbols and solid black lines represent the values and linear regression for the defaunated plots. The ratio of coarse: fine luminophores as a function of time. The open symbols and the dashed line represent the values and linear regression for the control plots, the solid black symbols and solid black line represent the values and linear regression for the defaunated plots.

tracer. Below this uniform layer, the amount of tracer fractions decreased exponentially as a function of sediment depth. The percentage of initial coarse tracer found in these deeper layers was 7%, against 1% of initial fine tracer.

In both the C and the NC cores we observed a decrease of tracer material from the sediment column as a whole during the experimental period. In the NC cores there was a decrease of 29% of coarse tracer and a 4% decrease of fine tracer (Table 3). In the C cores, we recorded a 37% decrease of coarse tracer and a 73% decrease of fine tracer material.

ANOVA (Time, Treatment and Fraction as factors, full factorial design) showed highly significant effects of Time, Treatment and Time × Treatment interaction ($p \ll 0.0001$, $p \ll 0.0001$, $p = 0.0007$, respectively), but no significant effect of either the factor Fraction or the Time × Fraction interaction ($p = 0.0915$, $p = 0.6791$, respectively). The Time × Treatment interaction and the Time - × Treatment × Fraction interaction both had a significant effect ($p = 0.0002$ and $p = 0.0018$, respectively). The resultant coarse:fine ratio decreased slightly between 0 and 21 days in the NC cores, whereas in the C cores, it increased almost two and a half times (Table 3).

4. Discussion

4.1. Luminophore use in bioturbation experiments

The two different luminophore size classes have proven to be very good visual tracers for bioturbation processes in the sediment. Both the direct profile-imaging as well as the budgeting of both fractions in the sediment column yielded valuable results and have improved our understanding on how benthic macrofauna can induce differential processing of sediment fractions, and its net effect on local vertical grain size distribution. Also, the luminophore layer in the defaunated plots enabled us to observe both gross and net effects of the absence of bioturbation; the actual amount and composition of accreted material on top of the layer could be measured directly.

The reported overlap in size distributions between the two luminophore types can be avoided by sieving them before application. We have not sieved the fractions due to logistical constraints, but in this case the overlap most probably reflected the natural situations where smaller particles can coagulate into larger flocs. Nevertheless, the use of two sizes of luminophores has been very successful in determining selectivity between sediment size fractions.

4.2. Macrobenthic assemblage

The defaunation treatment was very successful in the sense that we succeeded to create two very different macrofaunal assemblages with their respective bioturbatory effects to be studied. Within the experimental period of 32 days both the total macrofaunal density and the total macrofaunal biomass in the defaunated plots did not reach control levels, indicating that recolonisation has not reached its end-stage during the course of the experiment. In a parallel defaunation experiment in the same area both Van Colen et al. (2008) and Montserrat et al. (2008) described a rapid increase of microphytobenthos biomass (MPB; chl *a* data not shown here) and a quick but temporary recolonisation of mobile species, like the mudsnail *Hydrobia ulvae*, within the first month, whereas deeper burrowing macrofauna arrived only after two to three months.

Besides the mudsnail, the tellinid *Macoma balthica* and the polychaetes *Nereis diversicolor* and *Heteromastus filiformis* also colonised the defaunated plots in this study, but as these were all juvenile individuals – given their low biomass – their contribution to bioturbation processes within the experimental period can be considered marginal. *H. ulvae* is a highly mobile species, able to cover large distances (Andersen et al., 2002) while crawling over

Table 2
Parameter estimates and their respective standard errors for the minimal adequate model (MAM) obtained by analysis of covariance (ANCOVA) of the natural logarithm transformed luminophore fraction-specific pixel count for both treatments. See text for explanation on the ANCOVA and model derivation.

Parameter	Estimate	Std. Error	*p*
Intercept	3.767	0.096	≪0.0001
Time	−0.119	0.008	≪0.0001
Fraction	2.903	0.136	≪0.0001
Time × Treatment	0.091	0.01	≪0.0001
Time × Fraction	0.058	0.012	≪0.0001
Time × Treatment × Fraction	−0.033	0.014	0.0311

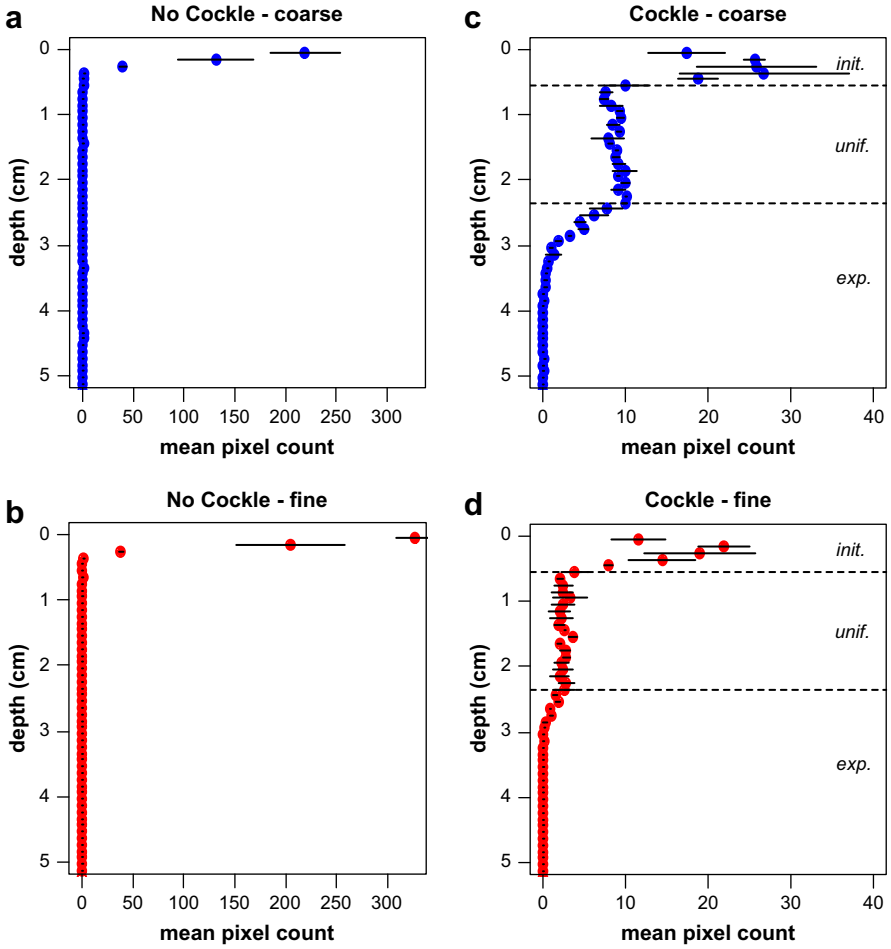

Fig. 8. The luminophore profiles, as a function of depth, of the cores used in the mesocosm experiment at $t = 21$ days. The dashed lines in the right-hand panels denote the three distinct layers the cockles have created through their movements (see text); "init.", initial luminophore layer; "unif.", uniformly mixed layer; "exp.", exponential decrease layer. Note the difference in scale along the *x*-axis (pixel count) between left- and right-hand panels. (a) No Cockle cores, coarse luminophores. (b) No Cockle cores, fine luminophores. (c) Cockle cores, coarse luminophores. (d) Cockle cores, fine luminophores.

the sediment surface and grazing on MPB. The recolonisation patterns observed in the first month by Van Colen et al. (2008) are therefore very similar to our recordings within the 32 days experimental period.

The macrofaunal assemblage in the control plots was dominated by *Cerastoderma edule* in terms of biomass and also, considering its shape, in terms of biovolume (Hillebrand et al., 1999 cited in Gilbert et al., 2007). *C. edule* is a motile, suspension feeding bivalve crawling through the top 3 cm of the sediment, able to affect both the biotic and abiotic parts of its environment (Ciutat et al., 2007; Flach, 1996; Montserrat et al., 2008). From earlier studies it has become clear that the effect of *C. edule* on the benthic boundary layer (BBL) is twofold: (1) the physical structure of its shell protruding from the sediment surface increases bottom roughness and (2) its movements cause biodestabilisation of the sediment surface. Both mechanisms were found to translate into a significant decrease of the U_{crit} (the critical erosion velocity – the velocity needed to erode 1 g of sediment m^{-2}) and a significantly higher sediment transport with an increase of animal density (Ciutat et al., 2007).

Following the classification used by Montserrat et al. (2008) to describe bioturbating fauna by their primary geomechanical effect, the macrofaunal assemblage at the Paulinapolder site – and therefore that in the control plots – was dominated by biodiffusors (*Cerastoderma edule*), with some contribution of gallery burrowers (*Nereis diversicolor*) and surface disruptors (*Macoma balthica*). Mentioned animals are well known to exert their main bioturbatory influences at the sediment surface layers (Gerino and Stora, 1991; Montserrat et al., 2008; Willows et al., 1998)

4.3. Tracer profiles and budgets

The apparent subsidence of the luminophore layer (Figs. 5a and 6a) was a very conspicuous effect of the absence of the natural assemblage and the concurrent lack of vertical sediment dynamics in the defaunated plots. In the absence of bioturbation, accretion of muddy sediment occurred in a linear fashion over time, causing downward advective transport of the luminophore layer. Once the luminophores in the defaunated plots were covered with a sufficiently thick layer of accreted sediment, they were not a part of the sediment–water interface anymore and thus unavailable for erosion by hydrodynamic processes. The luminophore layer itself remained relatively unchanged during the first samplings but was clearly subjected to advection/diffusion processes by the end of the experiment (Figs. 5a and 6a, b). Despite the diffusive processes, mainly mediated by recolonised juvenile fauna, the total amount of luminophores in the defaunated plots did not change much. The coarse luminophores virtually ceased to disappear from the sediment column after a week and between 65 and 70% was still present at the end of the experiment, whereas the fine tracer was continuously, albeit at a slow rate, removed from the sediment. However, both tracer fractions were overall more conserved in the defaunated sediment than in the non-treated controls.

Table 3
Depth-integrated luminophore fraction-specific mean ± SEM pixel counts for both treatments (NC and C) on both $t = 0$ days and $t = 21$ days. The coarse:fine luminophore ratio is stated in italics.

	0 Days coarse	Fine	Ratio	21 Days coarse	Fine	Ratio
No Cockle (NC)	561 ± 6	599 ± 6	*0.94*	400 ± 4	575 ± 6	*0.70*
Cockle (C)	504 ± 5	479 ± 5	*1.05*	320 ± 1	129 ± 1	*2.48*

In the control plots, the natural macrofaunal assemblage quickly reworked the tracers and relocated a portion to deeper sediment layers. Within the control treatment, there was some variation in the vertical distribution of the tracers between the two plots (Fig. 6c: 0 days [=1 h], 7 days and 32 days). This spatial variability in tracer distribution can be attributed to species known to be responsible for non-local transport, mainly *Macoma balthica* (Gingras et al., 2008; Michaud et al., 2006) and *Nereis diversicolor* (Duport et al., 2006; Fernandes et al., 2006). Lateral heterogeneity in bioturbation, which occurs typically over short time scales (Maire et al., 2007), may explain why the variation is found only in one plot or only during one sampling occasion.

4.4. Differential tracer processing

In the absence of macrofaunal bioturbators in the field experiment, there was accretion of mud, stabilisation of the accreted material and the sediment surface (Montserrat et al., 2008) and consequent subduction of the sediment tracers. In the control sediment we observed differential incorporation and processing of both tracer fractions. The data of these luminophore profiles could be used for estimating a biodiffusion coefficient (D_b) as a measure of sediment reworking rate at the community level. However useful, the use of biodiffusion models to estimate D_b should only be applied on larger spatial scales and, more important, longer temporal scales (Meysman et al., 2008a, b). The 32 days-lasting field experiment was simply too short of a period.

The presence of benthic animals in both the field and the mesocosm experiments caused differential incorporation of luminophores into the sediment but, more importantly, also a qualitatively high rate of resuspension. This resulted in the short-term loss of a significant amount of the luminophores. Even in the defaunated plots, there was loss of fine luminophores, but at a much lower rate than in the presence of a natural assemblage. The results from the field experiment are moreover well supported by the data from the mesocosm experiment. There was a significant higher loss of fine luminophores from the mesocosm cores, while still a high percentage of the coarse luminophores were retained, resulting in an increased coarse:fine ratio. We have shown here that the main effect of both the cockle-dominated natural assemblage and the cockles in the mesocosm experiment is selective removal of fine material from the sediment surface layers.

The selective removal of fines can be accomplished by the characteristic moving through the surface sediment layers or by the sudden adduction of the valves (respectively 'ploughing' and 'shaking') (Flach, 1996). Although *Cerastoderma edule* tends to have its natural abundance peak in fine to medium sands (Ysebaert et al., 2002), it does not directly utilise the bottom sediment and is therefore not dependent on its composition. However, cockles are negatively influenced by higher suspended sediment concentrations (SSC) to which they respond with a higher shaking frequency to get rid of fine material that clogs their gills (Ciutat et al., 2007).

We observed the shaking in the mesocosm experiment when the cockles were burrowing into the sediment as the water level receded. First, the agile foot was inserted into the sediment in a manner as described for crack propagation by burrowing marine polychaetes (Dorgan et al., 2005). The cockle then slowly opened its shell valves and adducted them quickly. In doing so, it forced the water from its mantle cavity and created a small body of fluidised sediment (quicksand) beneath its shell and, at almost the same moment, pulled itself down into the sediment with its foot. This was repeated until the cockle is burrowed beneath the sediment surface and only its siphons are visible. In nature, the burrowing behaviour of cockles causes sediment to become resuspended (more than is already caused by waves or valve adductions) of which the coarse fractions settle relatively fast. The fine fractions will be transported away by the overlying water, and might be captured from the water column by diatom mats (Austen et al., 1999; De Brouwer et al., 2003), vegetation (Bouma et al., 2005), reef-forming suspension feeders (Haven and Morales-Alamo, 1966) or dense aggregates of tubeworms (Montserrat et al., 2008).

4.5. Ecosystem engineering effects

Using the luminophore coarse:fine ratio as a proxy for the sediment sand:mud ratio, the cockle-dominated benthic assemblage's main effect was to render the sediment less muddy. The control sediment was characterised by a significantly higher erodability, compared to the situation without benthic fauna, in which net accretion of mud occurred. An increase in mud content, and the fact that it was not homogeneously mixed into the sediment by infauna as in a natural situation, can induce a local change in ecosystem functioning of the sediment through known biogeochemical cascades. First of all, a higher mud content entails a higher organic matter (OM) content with concomitant higher respiration rates (Aller and Aller, 1998). Secondly, the increased mud content decreases the permeability of the sediment and flow of pore water, decreasing the oxygen penetration depth (Winterwerp and Van Kesteren, 2004). Thirdly, a higher mud content will cause benthic primary production and standing stocks to increase (Van De Koppel et al., 2001). These profound changes would in turn reflect on the entire benthic community (micro-, meio- and macro-) and could have possibly set back the system to an earlier successional state (Connell and Slatyer, 1977; Pearson and Rosenberg, 1978; Van Colen et al., 2008).

Thrush et al. (2006) demonstrated the important structuring role of large surface-dwelling, suspension-feeding bivalves in the biogeochemistry and makeup of the macrobenthic assemblage in intertidal systems. Volkenborn et al. (2007b) attribute similar mechanisms to the lugworm *Arenicola marina* in the German Wadden Sea. *A. marina* is a model ecosystem engineer and has all the characteristics of a climax species: a long-lived, slow-growing, deep-burrowing, sediment-regenerating bioturbator (Riisgård and Banta, 1998), able to inhibit the settlement of other (pioneer) species (Flach, 1992) and even plants (Van Wesenbeeck et al., 2007). The physical restructuring of the bottom by its bioturbation increases the bottom roughness and resuspension of fine material, keeping the intertidal areas it inhabits more sandy (Volkenborn et al., 2007a). The influence *A. marina* exerts on the entire spectrum within the intertidal (grain size distribution – pore water flow – bacterial community – micro-/meio-/macrobenthos) enables it to maintain its habitat in a preferred state, which can abruptly change when it is excluded (Van De Koppel et al., 2001; Volkenborn et al., 2007a). The cockles in our experiment appear to fulfil a similar role in this particular system, including the inhibition of opportunist pioneer species (Bolam and Fernandes, 2003) and physical ecosystem engineering, through mechanical disturbance of the sediment.

The absence of the cockle-dominated assemblage in the defaunated plots made it clear that these animals and their behaviour can cause large differences in sediment behaviour

(Montserrat et al., 2008). As demonstrated in this study, the sediment erosion threshold during the first month was much higher in the defaunated plots than in the control plots. Although the sediment bed level of the defaunated plots increased slightly due to accumulation of muddy material, the difference was much less pronounced compared to a difference in the order of cm, observed in a parallel study by Montserrat et al. (2008). This can be unequivocally attributed to the fact that the recruitment peak of tube-building spionids, particularly *Pygospio elegans* (Claparède, 1863), did not occur due to the later initiation (i.e. opening of the plots) and the overall shorter duration of the experiment in this paper.

The lower abundance of grazing and mechanically disturbing fauna in the defaunated plots enabled MPB to form dense mats (Montserrat et al., 2008) which armour the sediment and can entrain mud. Constituting an important part of the macrobenthic assemblage, and backed up by the mesocosm experiment results, *Cerastoderma edule* was responsible for a large part of the bioturbatory effects in this system. This study has demonstrated that the burrowing and ploughing behaviour of these biodiffusing bivalves, often dominant species in intertidal sediments worldwide, is keeping the sediment matrix in a less muddy state – and therefore less organically enriched and less cohesive – by removing fine material from the sediment through an interaction of organism traits and hydrodynamic forcing.

5. Conclusions

(1) As true ecosystem engineers, cockles strongly shape their biotic and abiotic environment through a diverse array of effects which are specifically not trophic interactions, but are exerted via the environment.
(2) The presence of a healthy, fully developed macrofaunal community has a net erosive effect on muddy intertidal sediment. The net effect of the cockle-dominated macrofaunal assemblage, as well as the cockles in the mesocosm experiment, is mobilising surface sediment, resulting in a lower sediment erosion threshold.
(3) The burrowing behaviour of the cockles causes selective removal of fine material from the surface sediment, resulting in a shift in the sand:mud ratio. This shift can cause the sediment to become less cohesive, changing its erosion behaviour, biogeochemistry and ultimately its ecosystem functioning.

Acknowledgements

The authors would like thank Jos van Soelen, Bas Koutstaal and the masters' students who helped during the fieldwork and the processing of the samples for their efforts. Jon Marsh and several members of the team at Environmental Tracing Services helped us with advice on how to apply and process the luminophores, for which they have our thanks. This research is supported by the Dutch Technology Foundation STW, applied sciences division of NWO and the Technology Program of the Ministry of Economic Affairs. This is NIOO publication no. 4529.

References

Aller, R.C., 1994. Bioturbation and remineralization of sedimentary organic-matter – effects of redox oscillation. Chemical Geology 114, 331–345.
Aller, R.C., Aller, J.Y., 1998. The effect of biogenic irrigation intensity and solute exchange on diagenetic reaction rates in marine sediments. Journal of Marine Research 56, 905–936.
Andersen, T.J., Jensen, K.T., Lund-Hansen, L., Mouritsen, K.N., Pejrup, M., 2002. Enhanced erodibility of fine-grained marine sediments by *Hydrobia ulvae*. Journal of Sea Research 48, 51–58.
Andersen, T.J., Mikkelsen, O.A., Moller, A.L., Pejrup, M., 2000. Deposition and mixing depths on some European intertidal mudflats based on Pb-210 and Cs-137 activities. Continental Shelf Research 20, 1569–1591.
Austen, I., Andersen, T.J., Edelvang, K., 1999. The influence of benthic diatoms and invertebrates on the erodibility of an intertidal a mudflat, the Danish Wadden Sea. Estuarine, Coastal and Shelf Science 49, 99–111.
Bolam, S.G., Fernandes, T.F., 2003. Dense aggregations of *Pygospio elegans* (Claparede) effect on macrofaunal community structure and sediments. Journal of Sea Research 49, 171–185.
Borsje, B.W., De Vries, M.B., Huscher, S., De Boer, G.J., 2008. Modeling large-scale cohesive sediment transport affected by small-scale biological activity. Estuarine, Coastal and Shelf Science 78, 468–480.
Bouezmarni, M., Wollast, R., 2005. Geochemical composition of sediments in the Scheldt estuary with emphasis on trace metals. Hydrobiologia 540, 155–168.
Bouma, T.J., et al., 2005. Flow hydrodynamics on a mudflat and in salt marsh vegetation: identifying general relationships for habitat characterisations. Hydrobiologia 540, 259–274.
Caradec, S., Grossi, V., Hulth, S., Stora, G., Gilbert, F., 2004. Macrofaunal reworking activities and hydrocarbon redistribution in an experimental sediment system. Journal of Sea Research 52, 199–210.
Ciutat, A, Widdows, J., Pope, N.D., 2007. Effect of Cerastoderma edule density on near-bed hydrodynamics and stability of cohesive muddy sediments. Journal of Experimental Marine Biology and Ecology 346, 114–126.
Connell, J.H., Slatyer, R.O., 1977. Mechanisms of succession in natural communities and their role in community stability and organization. American Naturalist 111, 1119–1144.
Daborn, G.R., et al., 1993. An ecological cascade effect – migratory birds affect stability of intertidal sediments. Limnology and Oceanography 38, 225–231.
Dade, W.B., Nowell, A.R.M., Jumars, P.A., 1992. Predicting erosion resistance of muds. Marine Geology 105, 285–297.
De Brouwer, J.F.C., Neu, T.R., Stal, L.J., 2003. On the function of secretion of extracellular polymeric substances by benthic diatoms and their role in intertidal mudflats: a review of recent insights and views, p. 45–61. In: Kromkamp, J.C., De Brouwer, J.F.C., Blanchard, G.F., Forster, R.M., Creach, V. (Eds.), Microphytbenthos in Estuaries. Royal Netherlands Academy of Arts & Sciences (KNAW).
De Deckere, E.M.G.T., Van De Koppel, J., Heip, C.H.R., 2000. The influence of Corophium volutator abundance on resuspension. Hydrobiologia 426, 37–42.
Dorgan, K.M., Jumars, P.A., Johnson, B., Boudreau, B.P., Landis, E., 2005. Burrow extension by crack propagation. Nature 433, 475.
Duport, E., Gilbert, F., Poggiale, J.C., Dedieu, K., Rabouille, C., Stora, G., 2007. Benthic macrofauna and sediment reworking quantification in contrasted environments in the Thau Lagoon. Estuarine, Coastal and Shelf Science 72, 522–533.
Duport, E., Stora, G., Tremblay, P., Gilbert, F., 2006. Effects of population density on the sediment mixing induced by the gallery-diffusor *Hediste* (*Nereis*) *diversicolor* O.F. Muller, 1776. Journal of Experimental Marine Biology and Ecology 336, 33–41.
Fernandes, S., Meysman, F.J.R., Sobral, P., 2006. The influence of Cu contamination on Nereis diversicolor bioturbation. Marine Chemistry 102, 148–158.
Flach, E.C., 1992. Disturbance of benthic infauna by sediment-reworking activities of the Lugworm Arenicola-Marina. Netherlands Journal of Sea Research 30, 81–89.
Flach, E.C., 1996. The influence of the cockle, *Cerastoderma edule*, on the macrozoobenthic community of tidal flats in the Wadden Sea. Marine Ecology – Pubblicazioni Della Stazione Zoologica di Napoli I 17, 87–98.
Flemming, B.W., 2000. A revised textural classification of gravel-free muddy sediments on the basis of ternary diagrams. Continental Shelf Research 20, 1125–1137.
Gerino, M., 1990. The effects of bioturbation on particle redistribution in mediterranean coastal sediment – preliminary results. Hydrobiologia 207, 251–258.
Gerino, M., et al., 1998. Comparison of different tracers and methods used to quantify bioturbation during a spring bloom: 234-thorium, luminophores and chlorophyll a. Estuarine, Coastal and Shelf Science 46, 531–547.
Gerino, M., Stora, G., 1991. Invitro quantitative-analysis of the bioturbation induced by the polychaete *Nereis Diversicolor*. Comptes Rendus de l Academie des Sciences Serie Iii-Sciences de la Vie-Life Sciences 313, 489–494.
Gilbert, F., et al., 2007. Sediment reworking by marine benthic species from the Gullmar Fjord (Western Sweden): importance of faunal biovolume. Journal of Experimental Marine Biology and Ecology 348, 133–144.
Gingras, M.K., Pemberton, S.G., Dashtgard, S., Dafoe, L., 2008. How fast do marine invertebrates burrow? Palaeogeography, Palaeoclimatology, Palaeoecology 270, 280–286.
Haven, D.S., Morales-Alamo, R., 1966. Aspects of biodeposition by oysters and other invertebrate filter feeders. Limnology and Oceanography 11, 487.
Hedges, J.I., Keil, R.G., 1995. Sedimentary organic matter preservation: an assessment and speculative synthesis. Marine Chemistry 49, 81–115.
Hillebrand, H., Duerselen, C.D., Kirschtel, D., Pollinger, U., Zohary, T., 1999. Biovolume calculation for pelagic and benthic microalgae. Journal of Phycology 35, 403–424.
Le Hir, P., Monbet, Y., Orvain, F., 2007. Sediment erodability in sediment transport modelling: can we account for biota effects? Continental Shelf Research 27, 1116–1142.
Luckenbach, M.W., 1986. Sediment stability around animal tubes: the roles of hydrodynamic processes and biotic activity. Limnology and Oceanography 31, 779–787.
Mahaut, M.L., Graf, G., 1987. A luminophore tracer technique for bioturbation studies. Oceanologica Acta 10, 323–328.

Maire, O., Duchêne, J.C., Grémare, A., Malyuga, V.S., Meysman, F.J.R., 2007. A comparison of sediment reworking rates by the surface deposit-feeding bivalve *Abra ovata* during summertime and wintertime, with a comparison between two models of sediment reworking. Journal of Experimental Marine Biology and Ecology 343, 21–36.

Maire, O., Lecroart, P., Meysman, F., Rosenberg, R., Duchene, J.C., Gremare, A., 2008. Quantification of sediment reworking rates in bioturbation research: a review. Aquatic Biology 2, 219–238.

Meysman, F.J.R., Malyuga, V.S., Boudreau, B.P., Middelburg, J.J., 2008a. A generalized stochastic approach to particle dispersal in soils and sediments. Geochimica Et Cosmochimica Acta 72, 3460–3478.

Meysman, F.J.R., Malyuga, V.S., Boudreau, B.P., Middelburg, J.J., 2008b. Quantifying particle dispersal in aquatic sediments at short time scales: model selection. Aquatic Biology 2, 239–254.

Michaud, E., Desrosiers, G., Mermillod-Blondin, F., Sundby, B., Stora, G., 2006. The functional group approach to bioturbation: II. The effects of the *Macoma balthica* community on fluxes of nutrients and dissolved organic carbon across the sediment–water interface. Journal of Experimental Marine Biology and Ecology 337, 178–189.

Mitchener, H., Torfs, H., 1996. Erosion of sand/mud mixtures. Coastal Engineering 29, 1–25.

Montserrat, F., Van Colen, C., Degraer, S., Ysebaert, T., Herman, P.M.J., 2008. Benthic community-mediated sediment dynamics. Marine Ecology – Progress Series 372, 43–59.

Mulsow, S., Landrum, P.F., Robbins, J.A., 2002. Biological mixing responses to sublethal concentrations of DDT in sediments by *Heteromastus filiformis* using a Cs-137 marker layer technique. Marine Ecology – Progress Series 239, 181–191.

Nowell, A.R.M., Jumars, P.A., Eckman, J.E., 1981. Effects of biological-activity on the entrainment of marine-sediments. Marine Geology 42, 133–153.

Oost, A.P., 1995. Dynamics and Sedimentary Development of the Dutch Wadden Sea with Emphasis on the Frisian Inlet. Universiteit Utrecht.

Pearson, T.H., Rosenberg, R., 1978. Macrobenthic succession in relation to organic enrichment and pollution of the marine environment. Oceanography and Marine Biology Annual Review 16, 229–311.

Quinn, G.P., Keough, M.J., 2002. In: Experimental Design and Data Analysis for Biologists, first ed. Cambridge University Press.

Rhoads, D.C., 1974. Organism–sediment relations on the muddy sea floor. Oceanography and Marine Biology: An Annual Review 12, 263–300.

Rhoads, D.C., Young, D.K., 1970. The Influence of deposit-feeding organisms on sediment stability and community trophic structure. Journal of Marine Research 28, 150.

Riisgård, H.U., Banta, G.T., 1998. Irrigation and deposit feeding by the lugworm *Arenicola marina*, characteristics and secondary effects on the environment. A review of current knowledge. Vie et Milieu-Life and Environment 48, 243–257.

Sandnes, J., Forbes, T., Hansen, R., Sandnes, B., Rygg, B., 2000. Bioturbation and irrigation in natural sediments, described by animal-community parameters. Marine Ecology – Progress Series 197, 169–179.

Sistermans, W.C.H., et al., 2007. Het macrobenthos van de Westerschelde, de Oosterschelde, het Veerse Meer en het Grevelingenmeer in het voor – en najaar van 2006 (in Dutch). KNAW Netherlands Institute of Ecology – Centre for Estuarine and Marine Ecology, p. 133.

Solan, M., et al., 2004. In situ quantification of bioturbation using time-lapse fluorescent sediment profile imaging (f-SPI), luminophore tracers and model simulation. Marine Ecology – Progress Series 271, 1–12.

Thrush, S.F., Hewitt, J.E., Gibbs, M., Lundquist, C., Norkko, A., 2006. Functional role of large organisms in intertidal communities: community effects and ecosystem function. Ecosystems 9, 1029–1040.

Tolhurst, T.J., et al., 1999. Measuring the in situ erosion shear stress of intertidal sediments with the cohesive strength meter. Estuarine, Coastal and Shelf Science 49, 281–294.

Van Colen, C., Montserrat, F., Herman, P.M.J., Vincx, M., Ysebaert, T., Degraer, S., 2008. Macrobenthic recovery from hypoxia in an estuarine tidal mudflat. Marine Ecology – Progress Series 372, 31–42.

Van De Koppel, J., Herman, P.M.J., Thoolen, P., Heip, C.H.R., 2001. Do alternate stable states occur in natural ecosystems? Evidence from a tidal flat. Ecology 82, 3449–3461.

Van Duren, L.A., Herman, P.M.J., Sandee, A.J.J., Heip, C.H.R., 2006. Effects of mussel filtering activity on boundary layer structure. Journal of Sea Research 55, 3–14.

Van Ledden, M., 2003. Sand–mud segregation in estuaries and tidal basins. Communications on Hydraulic and Geotechnical Engineering. Delft University of Technology.

Van Ledden, M., Van Kesteren, W.G.M., Winterwerp, J.C., 2004. A conceptual framework for the erosion behaviour of sand-mud mixtures. Continental Shelf Research 24, 1–11.

Van Wesenbeeck, B.K., Van De Koppel, J., Herman, P.M.J., Bakker, J.P., Bouma, T.J., 2007. Biomechanical warfare in ecology; negative interactions between species by habitat modification. Oikos 116, 742–750.

Volkenborn, N., Hedtkamp, S.I.C., Van Beusekom, J.E.E., Reise, K., 2007a. Effects of bioturbation and bioirrigation by lugworms (*Arenicola marina*) on physical and chemical sediment properties and implications for intertidal habitat succession. Estuarine, Coastal and Shelf Science 74, 331–343.

Volkenborn, N., Polerecky, L., Hedtkamp, S.I.C., Van Beusekom, J.E.E., De Beer, D., 2007b. Bioturbation and bioirrigation extend the open exchange regions in permeable sediments. Limnology and Oceanography 52, 1898–1909.

Wheatcroft, R.A., Martin, W.R., 1996. Spatial variation in short-term (Th-234) sediment bioturbation intensity along an organic-carbon gradient. Journal of Marine Research 54, 763–792.

Wheatcroft, R.A., Olmez, I., Pink, F.X., 1994. Particle bioturbation in Massachusetts Bay – preliminary-results using a new deliberate tracer technique. Journal of Marine Research 52, 1129–1150.

Willows, R.I., Widdows, J., Wood, R.G., 1998. Influence of an infaunal bivalve on the erosion of an intertidal cohesive sediment: a flume and modeling study. Limnology and Oceanography 43, 1332–1343.

Winterwerp, J.C., Van Kesteren, W.G.M., 2004. In: Introduction to the Physics of Cohesive Sediment in the Marine Environment, first ed. Elsevier.

Ysebaert, T., Meire, P., Herman, P.M.J., Verbeek, H., 2002. Macrobenthic species response surfaces along estuarine gradients: prediction by logistic regression. Marine Ecology – Progress Series 225, 79–95.